ORIGINAL ARTICLE

Podoplanin: A Marker for Reactive Gliosis in Gliomas and Brain Injury

Kushal Kolar, Moises Freitas-Andrade, PhD, John F. Bechberger, MSc, Harini Krishnan, PhD,
Gary S. Goldberg, PhD, Christian C. Naus, PhD, and Wun Chey Sin, PhD

Abstract

Reactive astrogliosis is associated with many pathologic processes in the central nervous system, including gliomas. The glycoprotein podoplanin (PDPN) is upregulated in malignant gliomas. Using a syngeneic intracranial glioma mouse model, we show that PDPN is highly expressed in a subset of glial fibrillary acidic protein–positive astrocytes within and adjacent to gliomas. The expression of PDPN in tumor-associated reactive astrocytes was confirmed by its colocalization with the astrocytic marker S100β and with connexin43, a major astrocytic gap junction protein. To determine whether the increase in PDPN is a general feature of gliosis, we used 2 mouse models in which astrogliosis was induced either by a needle injury or ischemia and observed similar upregulation of PDPN in reactive astrocytes in both models. Astrocytic PDPN was also found to be coexpressed with nestin, an intermediate filament marker for neural stem/progenitor cells. Our findings confirm that expression of PDPN is part of the normal host response to brain injury and gliomas, and suggest that it may be a novel cell surface marker for a specific population of reactive astrocytes in the vicinity of gliomas and nonneoplastic brain lesions. The findings also highlight the heterogeneity of glial fibrillary acidic protein–positive astrocytes in reactive gliosis.

Key Words: Astrocyte, Connexin43, GFAP, Glioma, Gliosis, Ischemia, Podoplanin.

INTRODUCTION

Gliomas include the most aggressive forms of adult primary brain tumors (1, 2); they are characterized by high degrees of intratumoral heterogeneity that complicate their treatment (3, 4). The complex composition of glioma environments is also attributable to the presence of nontransformed central nervous system (CNS) resident cells within the tumors that may facilitate tumor progression, thereby affecting patient survival (5–7). Reactive astrocytes expressing increased levels of glial fibrillary acidic protein (GFAP) are found around gliomas (8–11); by the formation of glial scars, they can separate healthy CNS tissues from a variety of focal lesions (12–15).

Podoplanin (PDPN) is a mucin-type transmembrane glycoprotein that has been implicated in various cellular processes, including tumor migration and invasion (16–19); the mechanisms by which PDPN mediates its action are unclear, although it affects the activities of RhoA and ERM (Ezrin, Radixin, Moesin) proteins, which link cell membranes and the cytoskeleton (20). Much more is known about PDPN as a ligand for C-type lectin receptor CLEC-2 in platelet aggregation (21) and its association with the immune system (16).

Enhanced expression of PDPN has been associated with malignant progression of astrocytic tumors (22–24). In addition, PDPN is detected in glioma stem cells (25), which interact extensively with the tumor microenvironment (26). Podoplanin coexpressed with nestin, an embryonic intermediate filament that is re-expressed in reactive astrocytes (27–30). It also colocalized with connexin43 (Cx43), a gap junction protein that is expressed in neural progenitor cells (31, 32) and upregulated in reactive astrocytes induced by various brain injuries, including stab wounds (33–36). Recent evidence suggests that the glial scar contains a distinct population of reactive astrocytes that are derived from neural stem cells (37).

Here, we found that PDPN is highly expressed within some gliomas and in tissues adjacent to gliomas. Its upregulation in glioma-associated reactive astrocytes was demonstrated using a mouse model consisting of intracranial syngeneic implantation of mouse GL261 glioma cells. We further show that induction of PDPN is not attributable to the presence of glioma cells per se because increased PDPN was also observed in GFAP-positive astrocytes activated by stab wounds and ischemic injury. Our findings suggest that PDPN is a novel cell surface marker for reactive astrocytes with an expression profile that is associated with progenitor cells, raising the possibility that PDPN may have a role in providing a permissive environment for cellular regeneration after brain injury.

MATERIALS AND METHODS

Animals

Male and female mice were maintained in an animal facility with a 12-hour light/dark cycle and provided food and water ad libitum. All breeding and animal procedures were approved by The University of British Columbia Animal Care Committee and performed in accordance with the guidelines established by the Canadian Council on Animal Care.

Cell Line

Mouse GL261 glioma cells (NCI-Frederick Division of Cancer Treatment and Diagnosis, Frederick, MD) were maintained in Dulbecco modified Eagle medium supplemented with 10% fetal bovine serum and transfected with pcDNA-mCherry plasmid with Lipofectamine 2000 (Invitrogen, Carlsbad, CA).

Antibodies

The antibodies used for Western blot and immunofluorescence histochemistry were as follows: rabbit anti-Cx43 (C6219, 1:400 for immunofluorescence histochemistry; Sigma, St Louis, MO); mouse anti–glyceraldehyde 3-phosphate dehydrogenase (5G4 MAb 6C5, 1:5000 for Western blot; HyTest Ltd, Turku, Finland); mouse anti-GFAP (G3893, 1:600 for immunofluorescence histochemistry and 1:2000 for Western blot; Sigma); rabbit anti-IBA1 (1:400 for immunofluorescence histochemistry; Wako, Richmond, VA); mouse anti-nestin (rat-401, 1:85 for immunofluorescence histochemistry; Developmental Studies Hybridoma Bank, Iowa City, IA); hamster anti-PDPN (8.1.1, 1:200 for immunofluorescence histochemistry and 1:5000 for Western blot; Developmental Studies Hybridoma Bank) (38); rabbit anti-PDPN (SC-134483, 1:50 for immunofluorescence histochemistry; Santa Cruz Biotechnology, Santa Cruz, CA); rabbit anti-S100β (ab868, 1:200 for immunofluorescence histochemistry; Abcam, Cambridge, MA); and anti–RFP/mCherry (A00682, 1:750 for Western blot; Genscript, Piscataway, NJ).

Intracranial Implantation of Glioma Cells

Mice were anesthetized with isoflurane and a 1.0-mm-diameter hole was drilled through the skull. GL261 cells (2.5×10^4) were resuspended in 2 μL of Hanks balanced salt solution and injected intracerebrally with a 33-gauge syringe into the striatum of adult C57BL/6 mice at a position 2.5 mm lateral to the midline, 1.0 mm anterior to the bregma, and 3.0 mm ventral to the dura. At 7 or 14 days after injection, mice were killed and brains were fixed by transcardial perfusion with 4% paraformaldehyde in 0.1 mol/L of phosphate-buffered saline (PBS) before being removed and processed for immunofluorescence.

Intracerebral Needle Injury

Stab wounds were performed as previously described (33). Essentially, 2 μL of PBS was injected intracerebrally, and brains were removed at 6 days postinjury.

Middle Cerebral Artery Occlusion

The procedure was carried out as previously described (39). Briefly, an incision was made on the right side of the head of anesthetized 8-month-old mice, and the exposed middle cerebral artery was cauterized above and below the rhinal fissure using an electronic coagulator (Codman & Shurtleff, West Chester, PA). Mice were killed 4 or 6 days later for subsequent analysis.

Immunohistochemistry

Human brain tumor tissue microarray slides (GL208, GL2082, and GL2083; US Biomax, Rockville, MD) were probed with anti-PDPN antibody (D2-40, 1:100; BioLegend, San Diego, CA) and processed by Wax-it Histology Services Inc (Vancouver, British Columbia, CA), as previously described (40). Slides were scanned with an Aperio microscope scanner.

Immunofluorescence and Image Analysis

Sucrose-equilibrated brains were frozen in OCT compound (Tissue-Tek/Sakura, Torrance, CA) and sectioned at 10 μm thickness. Brain sections were blocked with 2% bovine serum albumin and 0.3% Triton X-100 in PBS and incubated sequentially with primary antibodies in 1% bovine serum albumin and 0.3% Triton X-100 at 4°C overnight and with corresponding Alexa Fluor secondary antibodies in 1% bovine serum albumin and 0.3% Triton X-100 at room temperature for 1 hour. Sections were mounted with Prolong Gold (Invitrogen) and imaged with a Leica TCS SP5 II Basic VIS system.

To quantify the extent of PDPN and GFAP staining from the tumor border or needle tract, we delineated the tumor border in ImageJ with reference to mCherry fluorescence or visually identified the needle tract. Images were adjusted by thresholding, and 20 to 30 measurements were performed around the tumor (from the delineated border or needle tract to the last point along each radius, where the proteins could be detected) as previously described (33). At least 3 animals were analyzed under each experimental condition.

Protein Extraction and Western Blot Analysis

Tumor samples were obtained by microdissection of fresh brain tissue from mice containing implanted GL261 cells. Tissue surrounding the stab wound and cortical tissues from mice subjected to middle cerebral artery occlusion (MCAO) were isolated from fresh frozen brain sections with a 25-gauge needle under a dissection microscope. Tissue samples were lysed in RIPA buffer containing 0.1% sodium dodecyl sulfate, 1% IGEPAL, 0.5% sarkosyl, 50 mmol/L of Tris-HCl (pH 8.0), and 150 mmol/L of NaCl supplemented with protease inhibitors (Roche Applied Science, Indianapolis, IN) and phosphatase inhibitors (Sigma). Protein concentrations were determined with a bicinchoninic acid assay kit before the separation of the protein lysate on a sodium dodecyl sulfate–polyacrylamide gel electrophoresis gel. After incubation of membranes with primary antibodies at 4°C overnight, they were rinsed and incubated with corresponding horseradish peroxidase–conjugated secondary antibodies (Sigma). Protein bands were detected with Amersham ECL Western detection reagents (GE Healthcare).

Statistical Analysis

To evaluate significance between 2 groups, we performed comparisons using Student *t*-test. $p < 0.05$ was considered significant. Data are presented as mean ± SE.

RESULTS

PDPN Is Expressed in Glioma-Associated Reactive Astrocytes

The presence of reactive astrocytes in brain lesions is usually confirmed by their enhanced GFAP immunoreactivity (8,14); a recent report has highlighted the possibility of stratifying Grade IV gliomas based on the expression of intermediate filament proteins (41). Expression of PDPN is significantly higher in malignant gliomas (22–24), and we similarly observed PDPN upregulation in Grade III and Grade IV glioma tissues when we probed a tissue tumor array for PDPN expression (Figure, Supplemental Digital Content 1, http://links.lww.com/NEN/A684). Interestingly, we observed PDPN staining in cell types resembling GFAP-positive astrocytes that were most obvious in Grade I and Grade II glioma tissues (Fig. 1A). Because PDPN expression has been detected in astrocytes (42–44), our results suggest
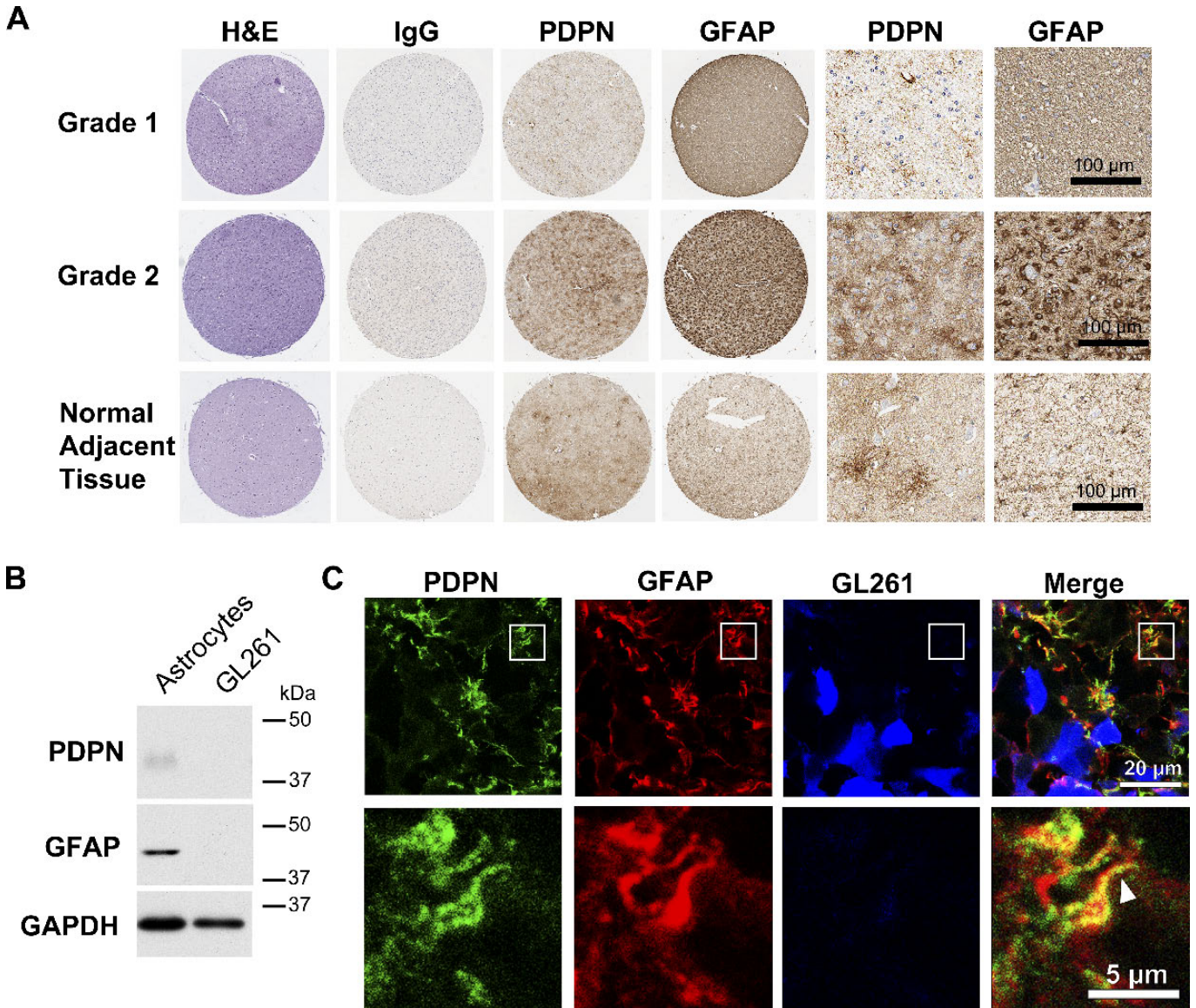

FIGURE 1. Expression of PDPN in primary low-grade human gliomas and adjacent tissues. **(A)** Representative images of 4 tumor cores (1 mm diameter) from Grade I and Grade II glioma samples. Images of hematoxylin and eosin (H&E) stains were obtained from US Biomax (http://www.biomax.us/). Podoplanin and GFAP immunoreactivity are visualized by brown staining. IgG served as negative control. Magnified images of PDPN and GFAP immunoreactivity are shown (two columns to the right of tumor cores). Structures resembling astrocyte processes in gliomas and adjacent normal tissues are PDPN-positive. **(B)** Western blot showing PDPN and GFAP expression in primary cultured mouse astrocytes and mouse GL261 glioma cells. GL261 cells express minimal levels of PDPN and GFAP in vitro. Glyceraldehyde 3-phosphate dehydrogenase (GAPDH) was used as loading control. **(C)** Coexpression of PDPN and GFAP in vivo in a 1-week-old GL261 tumor cell intracranial implant. mCherry-expressing glioma cells were pseudocolored in blue. Bottom panel shows the magnified image of the white box in the upper panel showing colocalization of PDPN and GFAP (white arrowhead).
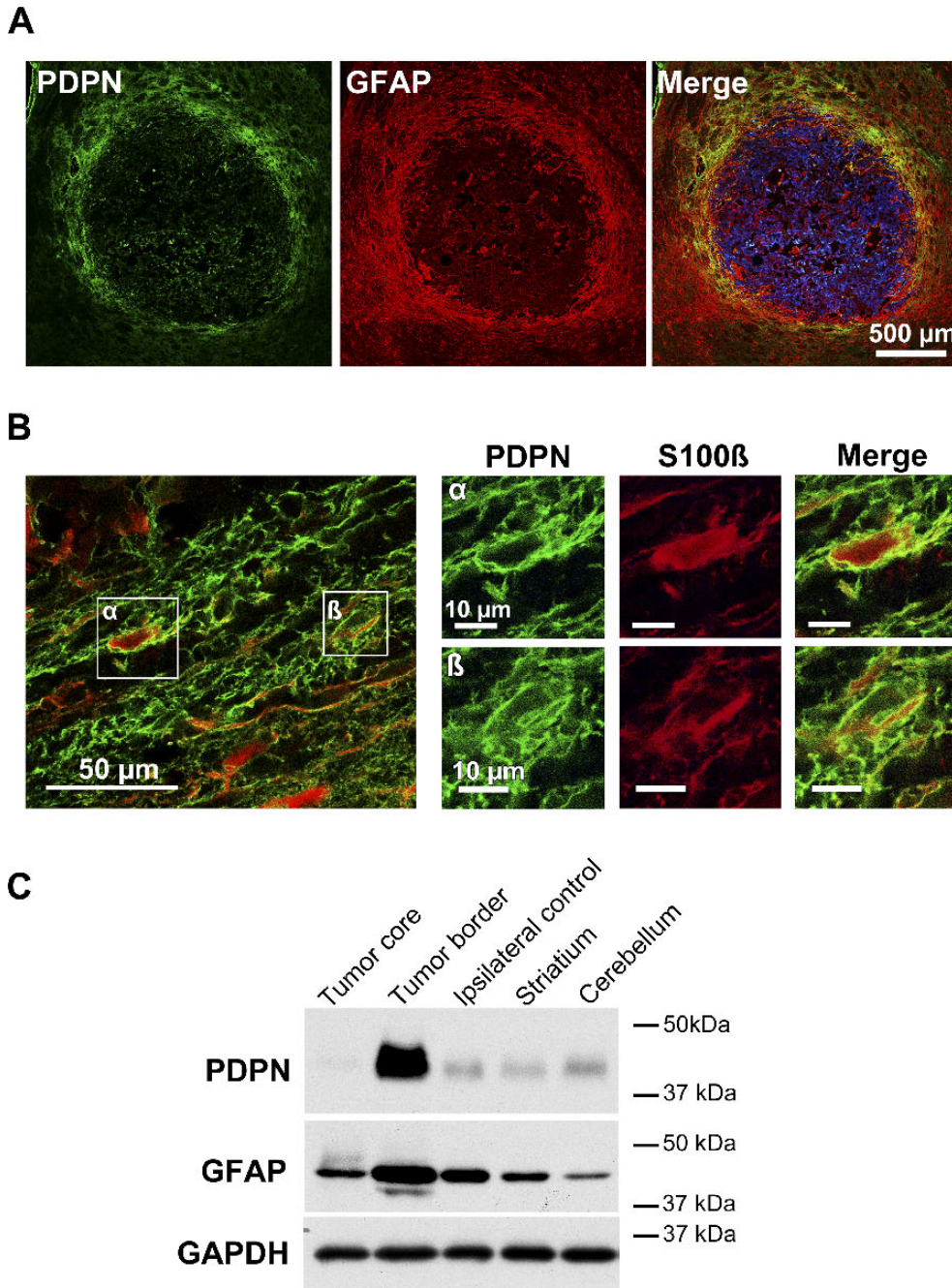
FIGURE 2. Upregulation of PDPN in reactive astrocytes at the glioma periphery. **(A)** Coexpression of PDPN and GFAP-positive reactive astrocytes at the tumor periphery. A glial scar formed around the implanted tumor at 2 weeks after intracranial implantation of GL261 cells. mCherry-expressing glioma cells were pseudocolored in blue. Glial fibrillary acidic protein immunofluorescence marks the region of gliosis. **(B)** Membrane-bound PDPN (green) surrounding S100β (red) at the tumor border. S100β is a cytosolic marker for astrocytes. Right panel shows the magnified image of white boxes α and β. **(C)** Western blot showing PDPN and GFAP expression in different mouse brain tissue samples obtained by microdissection. There is a noticeable increase in PDPN and GFAP protein levels in the tumor border sample compared to the core. Podoplanin is upregulated to a greater extent than GFAP. Glyceraldehyde 3-phosphate dehydrogenase (GAPDH) was used as loading control.

that some of the PDPN immunoreactivity in glioma tissues may be attributed to reactive astrocytes.

To confirm that PDPN is expressed in nonneoplastic glial cells, we used a mouse glioma cell line, GL261, that expresses minimal levels of endogenous PDPN and GFAP in vitro (Fig. 1B) in an intracranial animal model. We implanted mCherry-labeled GL261 cells into the striatum of syngeneic C57B/6 mice with an intact immune system (45, 46) and observed the expression of PDPN protein specifically in cells that did not express the fluorescent marker for transplanted

neoplastic cells (Fig. 1C). Using anti-GFAP antibody at a concentration that only detects reactive astrocytes (47, 48), we observed coexpression of GFAP and PDPN (Fig. 1C). This result was further supported by examination of PDPN expression in the glial scar, which was visualized as a region of enhanced GFAP expression caused by hypertrophy of astrocytes (14) at the glioma periphery (Fig. 2A). By costaining PDPN-labeled cells with anti-S100β (49), which is a cytoplasmic marker for astrocytes, we showed that PDPN is expressed in astrocytic glial cells; membrane-bound PDPN immunoreactivity surrounded cytoplasmic S100β in the same cells (Fig. 2B). Upregulation of PDPN protein at the tumor periphery was confirmed by Western blot analysis (Fig. 2C).

Consistent with immunofluorescence data, high PDPN expression was detected at the tumor border, and not in the tumor core, by Western blot (Fig. 2C). Upregulation of PDPN was greater than the corresponding upregulation of GFAP at the tumor border compared to the tumor core (Fig. 2C). In contrast, PDPN was not detected in IBA1-positive microglia, another major cell type found in the glioma microenvironment (Figure, Supplemental Digital Content 2, http://links.lww.com/NEN/A685) (5, 50).

Upregulation of astrocytic Cx43 has been detected in gliomas, particularly in the peritumoral region (51–53). Similar to PDPN, increased Cx43 immunoreactivity was observed in the brain parenchyma within 100 μm of the edge of the GL261 tumor mass (Fig. 3A). In addition, Western blot
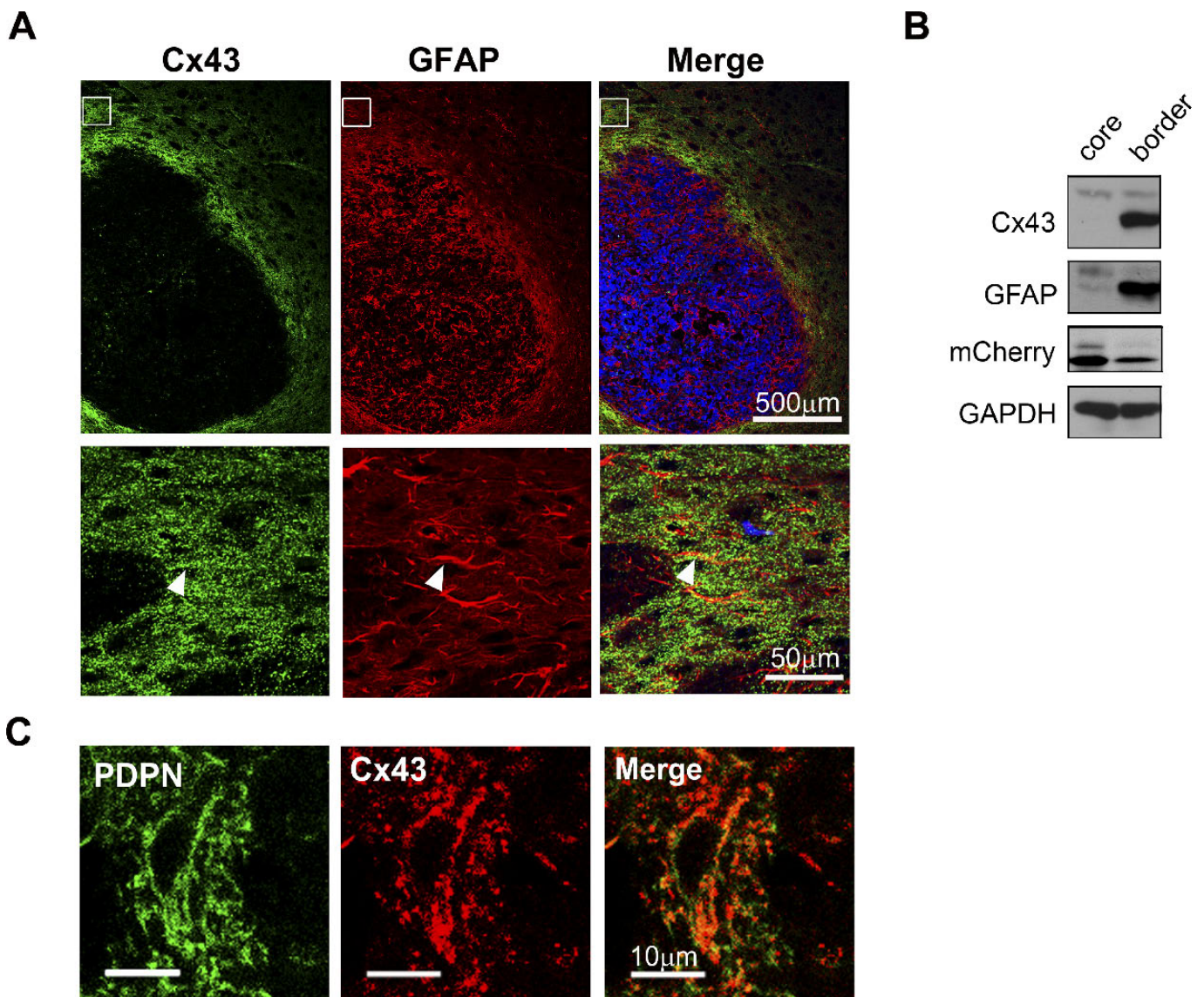

FIGURE 3. Colocalization of PDPN and Cx43 in tumor-associated reactive astrocytes. **(A)** Expression of Cx43 (green) and GFAP-positive reactive astrocytes (red) at the glioma periphery confirmed by co-immunostaining coronal brain sections with anti-Cx43 and anti-GFAP antibodies (white arrowheads). GL261 glioma cells were pseudocolored in blue. Bottom panel shows the magnified image of white boxes in the upper panel. **(B)** Western blot analysis with lysate from microdissected brain tissues. Co-upregulation of Cx43 and GFAP proteins at the tumor border compared to the core. Glyceraldehyde 3-phosphate dehydrogenase (GAPDH) was used as loading control. **(C)** Colocalization of PDPN and Cx43 in reactive astrocytes at the tumor border.

analysis of proteins isolated from microdissected tissue showed coexpression of Cx43 and GFAP at the glioma periphery, which is identified by its minimal mCherry level compared to the tumor core (Fig. 3B). Therefore, colocalization of Cx43 with PDPN (Fig. 3C) indicates that these proteins are expressed simultaneously in tumor-associated astrocytes adjacent to the mCherry-labeled GL261 glioma periphery.

PDPN Is Expressed in a Subset of Reactive Astrocytes Closest to the Tumor Periphery

Glial fibrillary acidic protein immunoreactivity has been widely used to assess the extent of gliosis under various pathologic conditions in the CNS (8, 14). We noticed that not all GFAP-expressing astrocytes were PDPN-positive in gliomas (Fig. 1A) and adjacent to implanted gliomas (Fig. 4A). Although the intensity of GFAP immunoreactivity reduced gradually until it was undetectable (429.9 ± 14.5 μm from the tumor border), PDPN staining diminished sharply (96.1 ± 4.2 μm from the tumor periphery) (Fig. 4B). These observations suggest the selective upregulation of PDPN in a subset of reactive astrocytes, indicating that a heterogeneous population of astrocytes comprises peritumoral tissue.

Upregulation of PDPN in Reactive Astrocytes Induced by Mechanical and Ischemic Injuries

To determine whether gliosis-induced PDPN upregulation is a host response independent of glioma cells, we first examined the expression of PDPN in astrocytes activated by a stab wound. The extent of astrogliosis, as visualized by enhanced GFAP and Cx43 immunoreactivity, peaked at 6 days postinjury (33). Using a stab wound injury model that we have previously established (33), we observed a significant increase in PDPN staining within a distance of 100 μm from the stab wound (Fig. 5A). In contrast, GFAP-positive astrocytes were more dispersed and detected at a considerably farther distance from the stab wound (Fig. 5A). Upregulation of PDPN within the region surrounding the stab wound, compared to the same region in the contralateral hemisphere, was confirmed by Western blot analysis of microdissected mouse brain tissues (Fig. 5B). Similar to our observation in gliosis induced by glioma, coexpression of PDPN and GFAP was also detected in gliosis induced by a mechanical stab wound (Figure, Supplemental Digital Content 3, A, B, http://links.lww.com/NEN/A686).

We next investigated whether there is a similar increase in PDPN levels in reactive astrocytes induced by MCAO. In agreement with previous studies (39, 54), there was a significant increase in GFAP immunoreactivity in the peri-infarct region surrounding dead tissue at 4 days postinjury (Fig. 6A). In contrast, upregulation of PDPN protein was more subtle (Fig. 6A). Although the temporal profile of MCAO-induced astrogliosis is not known, we speculate that maximal astrogliosis is unlikely to occur at 4 days postinjury (55, 56). Based on our results from stab wound–induced astrogliosis (33), we examined MCAO-induced PDPN expression at 6 days postinjury and observed a dramatic increase in PDPN expression in the peri-infarct region (Fig. 6A). The upregulation of PDPN in reactive astrocytes was confirmed by its colocalization with S100β

(Fig. 6B) and its coexpression with GFAP (Figure, Supplemental Digital Content 3, C, http://links.lww.com/NEN/A686). The differential upregulation of GFAP and PDPN in the ipsilateral ischemic hemisphere was also confirmed by Western blot analysis with microdissected brain tissues (Figure, Supplemental Digital Content 4, http://links.lww.com/NEN/A687).

Expression of PDPN in Nestin-Positive Reactive Astrocytes

Connexin43 colocalizes with nestin, which is re-expressed in reactive astrocytes (29,57–59). Using double immunofluorescence staining, we observed that PDPN colocalized with nestin in some reactive astrocytes (Fig. 7).

DISCUSSION

Astrocytes become ''reactive'' in response to neuronal death (12). At the molecular level, a specific set of proteins is upregulated in these astrocytes, although the significance of their increased expression remains unclear (42–44). In this
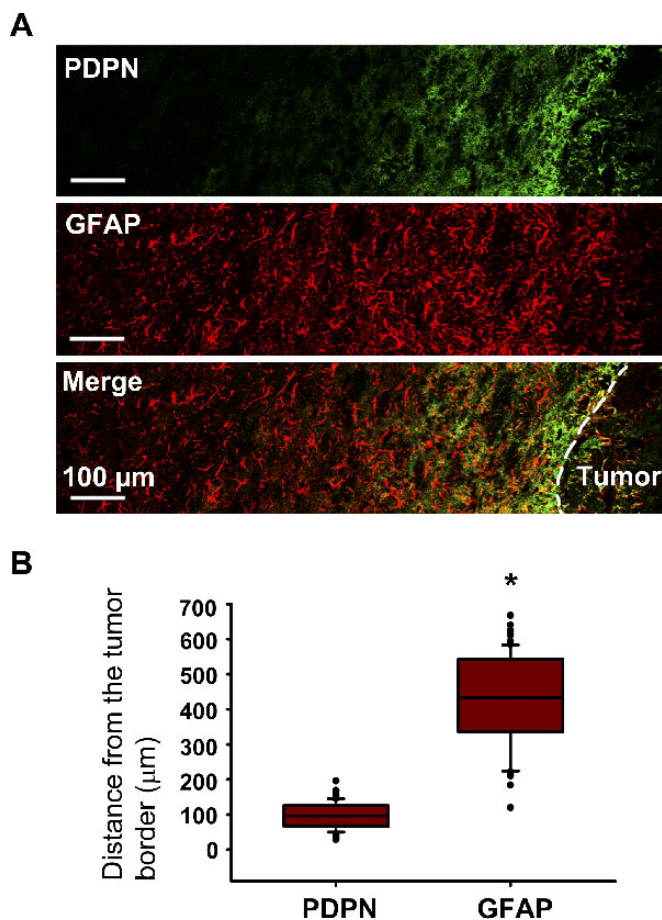

FIGURE 4. Expression of PDPN in a subset of reactive astrocytes closest to the tumor. **(A)** Immunofluorescence image showing PDPN immunostaining close to the tumor border (white dotted line) and sharply diminishing with distance. Glial fibrillary acidic protein (GFAP) expression is observed farther away from the tumor border. **(B)** Box plots representing the maximal distance of detectable PDPN and GFAP expression. * p = 0.0026 (Student *t*-test).
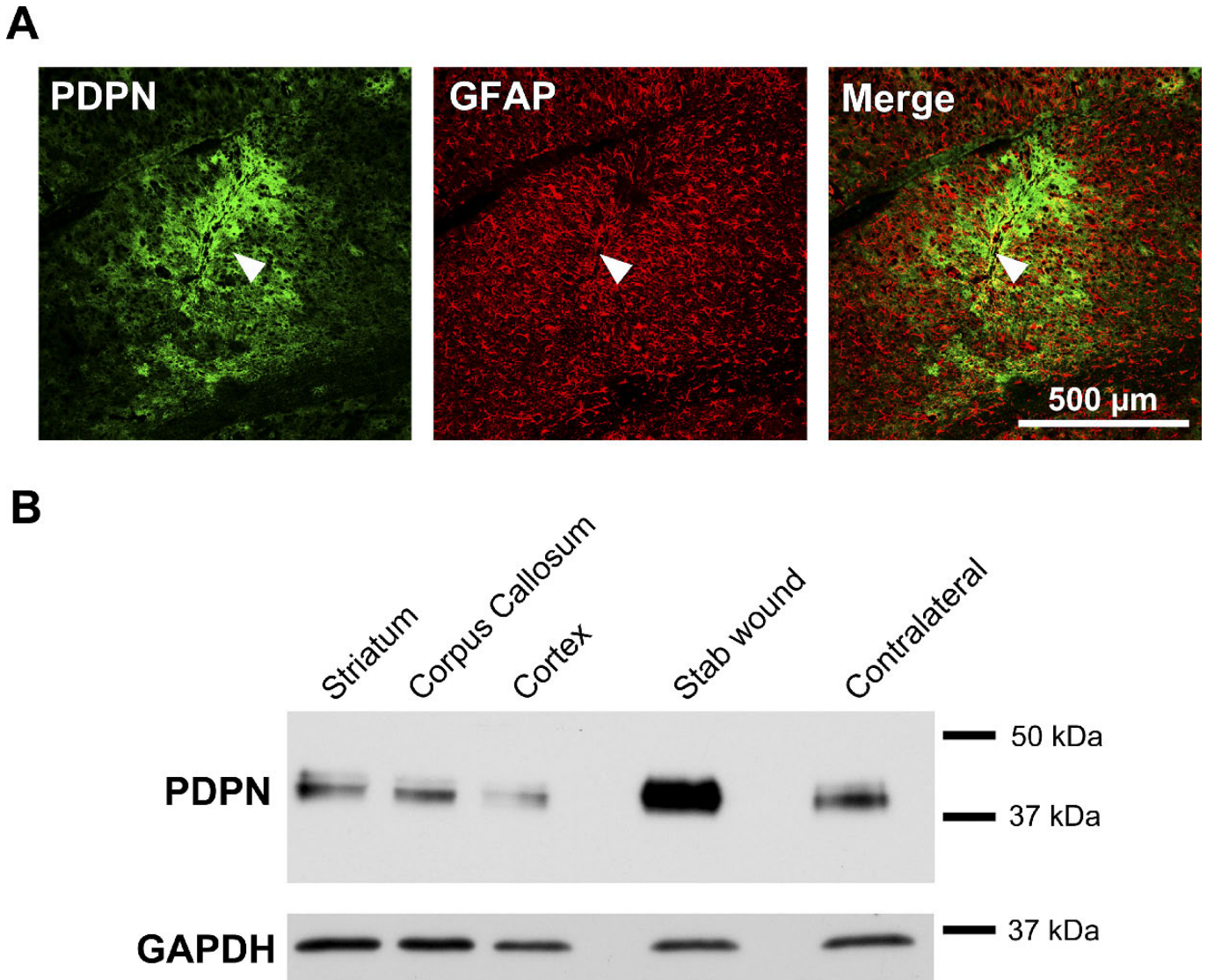
A

B

FIGURE 5. Upregulation of PDPN protein in reactive astrocytes induced by a mechanical stab wound. **(A)** Podoplanin is upregulated up to 100 μm from the needle tract (white arrowhead). The region of gliosis is highlighted by GFAP immunoreactivity. **(B)** Western blot analysis of cell lysate from microdissected brains showing the upregulation of PDPN protein (2.5-fold, as measured by Image J) in the stab wound compared to the same region in the contralateral side; this side shows a basal level of PDPN similar to that in the striatum, corpus callosum, and cortex of a noninjured brain. Glyceraldehyde 3-phosphate dehydrogenase (GAPDH) served as loading control.

regard, GFAP is the most widely used marker for reactive astrocytes (48, 60, 61), and its absence seems to attenuate astrogliosis (62). A genomic analysis reveals that astrocytes in reactive gliosis are highly heterogeneous and that distinct subsets of proteins are altered in response to specific injuries (63). Here, we demonstrate for the first time that PDPN expression is increased in astrocytes activated by glioma growth, mechanical stab wound, and brain ischemia.

Reactive astrogliosis serves to protect neurons from further damage, although it also inhibits their regeneration (13). Recent evidence reveals that the glial scar formed after spinal cord injury contains a distinct neural stem cell progeny adjacent to the lesion, and these cells exert a neuroprotective effect (64, 65). Moreover, cerebral infarction induces a subset of astrocytes with stem cell–like characteristics and the ability to form neurons (66, 67). We found that PDPN is upregulated in a subset of GFAP-positive reactive astrocytes that are proximal to a cerebral infarct. Podoplanin has been detected in stem cells (25, 68, 69); its colocalization with Cx43, which is also expressed in neural stem cells (32, 70,71), suggests that PDPN is a novel marker for detecting a specific subpopulation of reactive astrocytes. Furthermore, the coexpression of PDPN with nestin suggests that PDPN is expressed in reactive astrocytes with proliferative potential (29, 65, 72–74); therefore, the temporal expression of PDPN in ischemic brain suggests that it may play a role in recovery after the initial cellular insult.

Astrogliosis is a prominent feature of gliomas (10, 11, 75), and it is often difficult to distinguish glioma cells from reactive
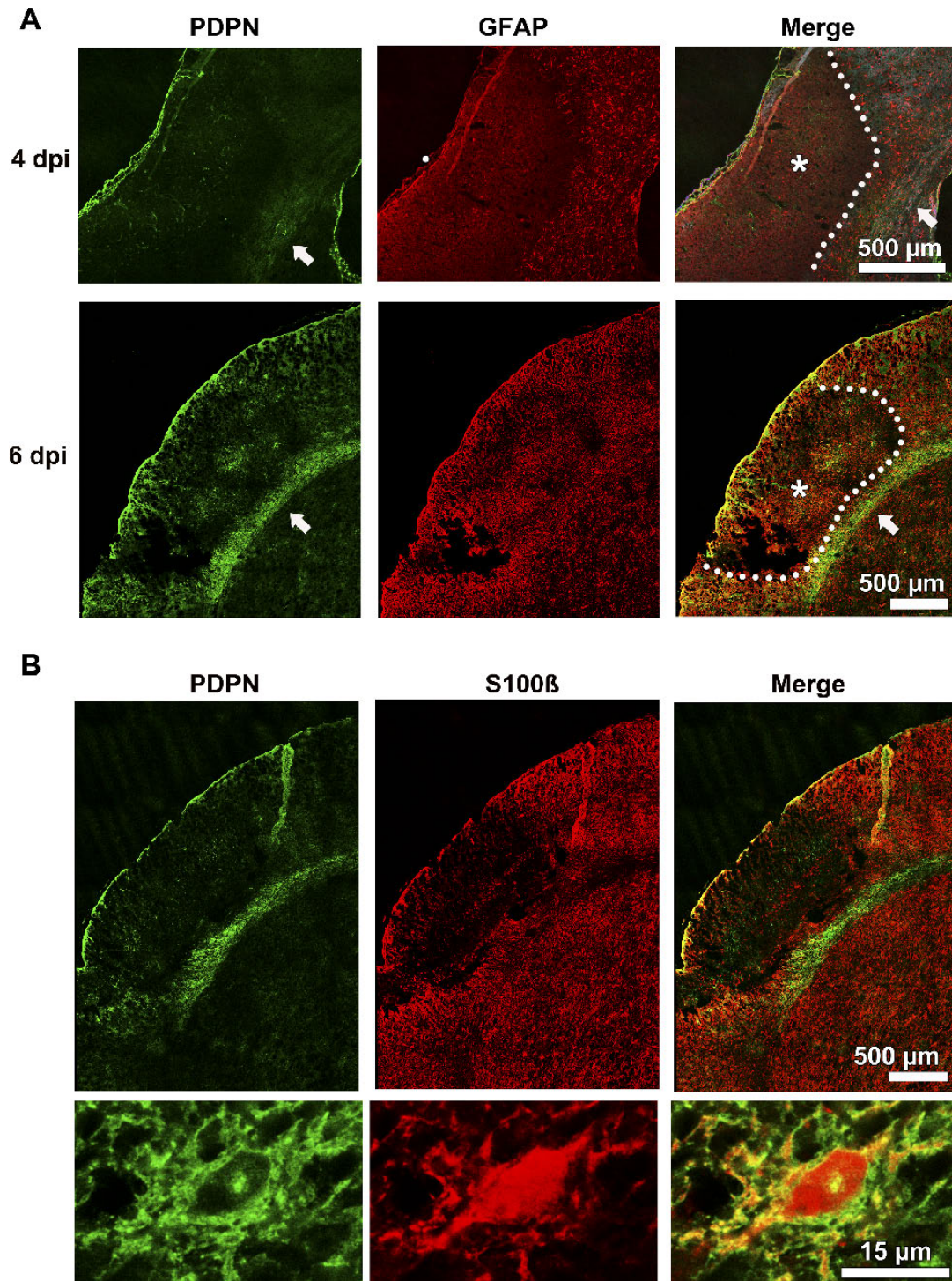
FIGURE 6. Increased PDPN expression in reactive astrocytes adjacent to ischemic infarcts. **(A)** Images of coronal brain sections showing enhanced GFAP staining surrounding the infarct region (white dotted line), with minimal GFAP immunoreactivity within the infarct core (*) after MCAO-induced ischemic infarct at 4 and 6 days postinjury. Podoplanin expression (green) is increased in the peri-infarct region at 6 days postinjury (white arrows). **(B)** Colocalization of PDPN (green) with the astrocyte marker S100β (red) in the peri-infarct region at 6 days postinjury.

astrocytes (75). An increase in PDPN expression has been reported in malignant gliomas (22–24), and our study suggests that a significant proportion of PDPN detected in gliomas may be attributed to tumor-associated reactive astrocytes. Therefore, our findings may explain why PDPN is not a useful diagnostic marker for grading glioma malignancy (24). The selective upregulation of PDPN and Cx43 in reactive astrocytes adjacent to glioma cells at the tumor-host interface implicates a role for
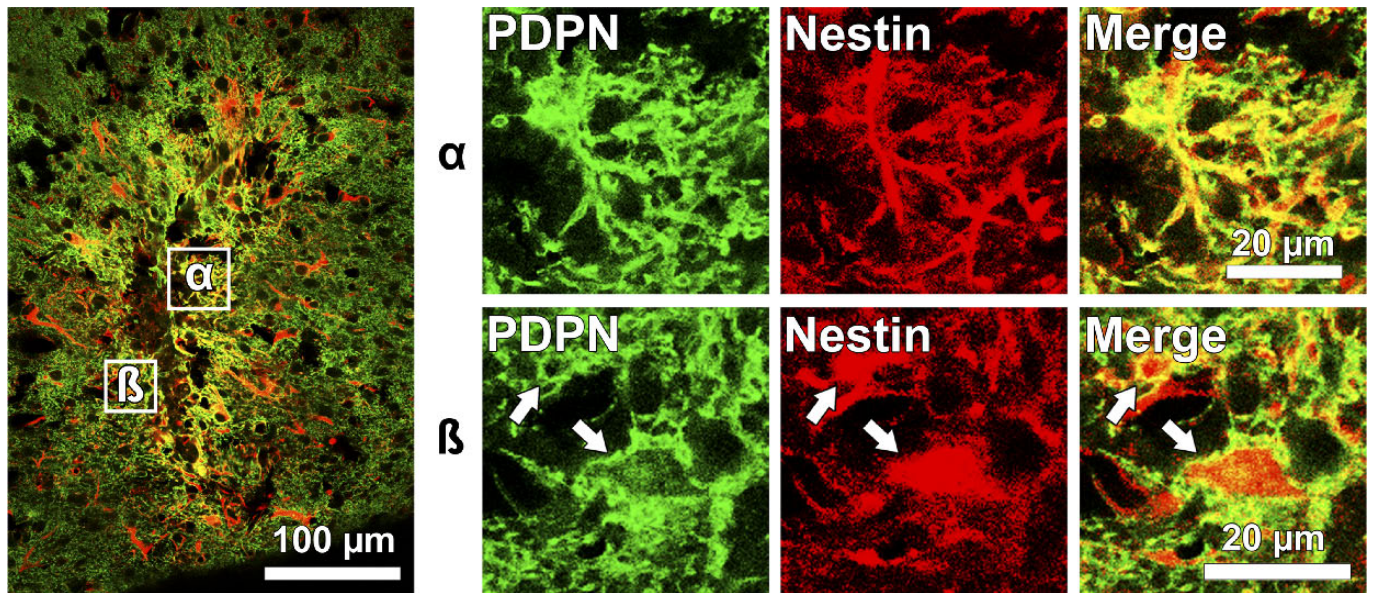
FIGURE 7. Expression of PDPN in nestin-positive reactive astrocytes. Colocalization of membrane-bound PDPN with nestin intermediate filaments (white arrows). Right panel shows the magnified images in white boxes α and β.

PDPN in microenvironment signaling at the invasive niche. In addition, some evidence suggests that progenitor cells have a major role in glioma progression and in the resistance of tumors to anticancer therapies (76, 77). Indeed, expression of PDPN in cancer-associated fibroblasts has been shown to enhance tumor progression in peripheral cancers (78–80). Podoplanin has become a promising target for chemotherapy for a variety of cancers, including gliomas (81–84). Accordingly, anti-PDPN antibody has been investigated for its feasibility to target malignant gliomas (83). Taken together, our findings highlight an unexplored role for PDPN in reactive gliosis, which is prominent in the glioma microenvironment and in brain injury.

ACKNOWLEDGMENTS

REFERENCES

1. Jones TS, Holland EC. Standard of care therapy for malignant glioma and its effect on tumor and stromal cells. Oncogene 2012;31:1995–2006
2. Holland EC. Glioblastoma multiforme: The terminator. Proc Natl Acad Sci USA 2000;97:6242–44
3. Sottoriva A, Spiteri I, Piccirillo SG, et al. Intratumor heterogeneity in human glioblastoma reflects cancer evolutionary dynamics. Proc Natl Acad Sci USA 2013;110:4009–14
4. Swanton C. Intratumor heterogeneity: Evolution through space and time. Cancer Res 2012;72:4875–82
5. Charles NA, Holland EC, Gilbertson R, et al. The brain tumor microenvironment. Glia 2011;59:1169–80
6. Joyce JA, Pollard JW. Microenvironmental regulation of metastasis. Nat Rev Cancer 2009;9:239–52
7. Hu M, Polyak K. Microenvironmental regulation of cancer development. Curr Opin Genet Dev 2008;18:27–34
8. Sofroniew MV, Vinters HV. Astrocytes: Biology and pathology. Acta Neuropathol 2010;119:7–35
9. Pekny M, Nilsson M. Astrocyte activation and reactive gliosis. Glia 2005;50:427–34
10. Katz AM, Amankulor NM, Pitter K, et al. Astrocyte-specific expression patterns associated with the PDGF-induced glioma microenvironment. PLoS One 2012;7:e32453
11. Lee J, Borboa AK, Baird A, et al. Non-invasive quantification of brain tumor–induced astrogliosis. BMC Neurosci 2011;12:9
12. Burda JE, Sofroniew MV. Reactive gliosis and the multicellular response to CNS damage and disease. Neuron 2014;81:229–48
13. Pekny M, Wilhelmsson U, Pekna M. The dual role of astrocyte activation and reactive gliosis. Neurosci Lett 2014;565C:30–38
14. Sofroniew MV. Molecular dissection of reactive astrogliosis and glial scar formation. Trends Neurosci 2009;32:638–47
15. Ridet JL, Malhotra SK, Privat A, et al. Reactive astrocytes: Cellular and molecular cues to biological function. Trends Neurosci 1997;20:570–77
16. Astarita JL, Acton SE, Turley SJ. Podoplanin: Emerging functions in development, the immune system, and cancer. Front Immunol 2012;3:283
17. Wicki A, Christofori G. The potential role of podoplanin in tumour invasion. Br J Cancer 2007;96:1–5
18. Martin-Villar E, Fernandez-Munoz B, Parsons M, et al. Podoplanin associates with CD44 to promote directional cell migration. Mol Biol Cell 2010;21:4387–99
19. Wicki A, Lehembre F, Wick N, et al. Tumor invasion in the absence of epithelial-mesenchymal transition: Podoplanin-mediated remodeling of the actin cytoskeleton. Cancer Cell 2006;9:261–72
20. Martin-Villar E, Megias D, Castel S, et al. Podoplanin binds ERM proteins to activate RhoA and promote epithelial-mesenchymal transition. J Cell Sci 2006;119:4541–53
21. Lowe KL, Navarro-Nunez L, Watson SP. Platelet CLEC-2 and podoplanin in cancer metastasis. Thromb Res 2012;129(Suppl 1):S30–37
22. Scrideli CA, Carlotti CG Jr, Okamoto OK, et al. Gene expression profile analysis of primary glioblastomas and non-neoplastic brain tissue: Identification of potential target genes by oligonucleotide microarray and real-time quantitative PCR. J Neurooncol 2008;88:281–91
23. Mishima K, Kato Y, Kaneko MK, et al. Increased expression of podoplanin in malignant astrocytic tumors as a novel molecular marker of malignant progression. Acta Neuropathol 2006;111:483–88
24. Shibahara J, Kashima T, Kikuchi Y, et al. Podoplanin is expressed in subsets of tumors of the central nervous system. Virchows Arch 2006;448:493–99
25. Ernst A, Hofmann S, Ahmadi R, et al. Genomic and expression profiling of glioblastoma stem cell–like spheroid cultures identifies novel tumor-relevant genes associated with survival. Clin Cancer Res 2009;15:6541–50

26. Lathia JD, Heddleston JM, Venere M, et al. Deadly teamwork: Neural cancer stem cells and the tumor microenvironment. Cell Stem Cell 2011;8:482–85

27. Krum JM, Rosenstein JM. Transient coexpression of nestin, GFAP, and vascular endothelial growth factor in mature reactive astroglia following neural grafting or brain wounds. Exp Neurol 1999;160:348–60

28. Li Y, Chopp M. Temporal profile of nestin expression after focal cerebral ischemia in adult rat. Brain Res 1999;838:1–10

29. Duggal N, Schmidt-Kastner R, Hakim AM. Nestin expression in reactive astrocytes following focal cerebral ischemia in rats. Brain Res 1997; 768:1–9

30. Frisen J, Johansson CB, Torok C, et al. Rapid, widespread, and longlasting induction of nestin contributes to the generation of glial scar tissue after CNS injury. J Cell Biol 1995;131:453–64

31. Duval N, Gomes D, Calaora V, et al. Cell coupling and Cx43 expression in embryonic mouse neural progenitor cells. J Cell Sci 2002;115: 3241–51

32. Bittman KS, LoTurco JJ. Differential regulation of connexin 26 and 43 in murine neocortical precursors. Cereb Cortex 1999;9:188–95

33. Theodoric N, Bechberger JF, Naus CC, et al. Role of gap junction protein connexin43 in astrogliosis induced by brain injury. PLoS One 2012;7:e47311

34. Lee IH, Lindqvist E, Kiehn O, et al. Glial and neuronal connexin expression patterns in the rat spinal cord during development and following injury. J Comp Neurol 2005;489:1–10

35. Fonseca CG, Green CR, Nicholson F. Upregulation in astrocytic connexin 43 gap junction levels may exacerbate generalized seizures in mesial temporal lobe epilepsy. Brain Res 2002;929:105–16

36. Hossain MZ, Peeling J, Sutherland GR, et al. Ischemia-induced cellular redistribution of the astrocytic gap junctional protein connexin43 in rat brain. Brain Res 1994;652:311–22

37. Cregg JM, DePaul MA, Filous AR, et al. Functional regeneration beyond the glial scar. Exp Neurol 2014;253:197–207

38. Shen Y, Chen CS, Ichikawa H, et al. SRC induces podoplanin expression to promote cell migration. J Biol Chem 2010;285:9649–56

39. Kozoriz MG, Bechberger JF, Bechberger GR, et al. The connexin43 C-terminal region mediates neuroprotection during stroke. J Neuropathol Exp Neurol 2010;69:196–206

40. Gielen PR, Aftab Q, Ma N, et al. Connexin43 confers temozolomide resistance in human glioma cells by modulating the mitochondrial apoptosis pathway. Neuropharmacology 2013;75:539–48

41. Skalli O, Wilhelmsson U, Orndahl C, et al. Astrocytoma grade IV (glioblastoma multiforme) displays 3 subtypes with unique expression profiles of intermediate filament proteins. Hum Pathol 2013;44:2081–88

42. Cahoy JD, Emery B, Kaushal A, et al. A transcriptome database for astrocytes, neurons, and oligodendrocytes: A new resource for understanding brain development and function. J Neurosci 2008;28:264–78

43. Doyle JP, Dougherty JD, Heiman M, et al. Application of a translational profiling approach for the comparative analysis of CNS cell types. Cell 2008;135:749–62

44. Lovatt D, Sonnewald U, Waagepetersen HS, et al. The transcriptome and metabolic gene signature of protoplasmic astrocytes in the adult murine cortex. J Neurosci 2007;27:12255–66

45. Jacobs VL, Valdes PA, Hickey WF, et al. Current review of in vivo GBM rodent models: Emphasis on the CNS-1 tumour model. ASN Neuro 2011;3:e00063

46. Newcomb E, Zagzag D. The murine GL261 glioma experimental model to assess novel brain tumor treatments. In: Meir EG, ed. CNS Cancer. Atlanta, GA: Humana Press, 2009;227–41

47. Schmidt-Kastner R, Wietasch K, Weigel H, et al. Immunohistochemical staining for glial fibrillary acidic protein (GFAP) after deafferentation or ischemic infarction in rat visual system: Features of reactive and damaged astrocytes. Int J Dev Neurosci 1993;11:157–74

48. Hozumi I, Chiu FC, Norton WT. Biochemical and immunocytochemical changes in glial fibrillary acidic protein after stab wounds. Brain Res 1990;524:64–71

49. Cerutti SM, Chadi G. S100 immunoreactivity is increased in reactive astrocytes of the visual pathways following a mechanical lesion of the rat occipital cortex. Cell Biol Int 2000;24:35–49

50. Graeber MB, Scheithauer BW, Kreutzberg GW. Microglia in brain tumors. Glia 2002;40:252–59

51. Baklaushev VP, Yusubalieva GM, Tsitrin EB, et al. Visualization of connexin 43–positive cells of glioma and the periglioma zone by means of intravenously injected monoclonal antibodies. Drug Deliv 2011;18: 331–37

52. Caltabiano R, Torrisi A, Condorelli D, et al. High levels of connexin 43 mRNA in high grade astrocytomas. Study of 32 cases with in situ hybridization. Acta Histochem 2010;112:529–35

53. Aronica E, Gorter JA, Jansen GH, et al. Expression of connexin 43 and connexin 32 gap-junction proteins in epilepsy-associated brain tumors and in the perilesional epileptic cortex. Acta Neuropathol (Berl) 2001; 101:449–59

54. Nakase T, Fushiki S, Naus CC. Astrocytic gap junctions composed of connexin 43 reduce apoptotic neuronal damage in cerebral ischemia. Stroke 2003;34:1987–93

55. Schwartz M, Baruch K. The resolution of neuroinflammation in neurodegeneration: Leukocyte recruitment via the choroid plexus. EMBO J 2014;33:7–22

56. Robel S, Berninger B, Gotz M. The stem cell potential of glia: Lessons from reactive gliosis. Nat Rev Neurosci 2011;12:88–104

57. Tamagno I, Schiffer D. Nestin expression in reactive astrocytes of human pathology. J Neurooncol 2006;80:227–33

58. Kronenberg G, Wang LP, Synowitz M, et al. Nestin-expressing cells divide and adopt a complex electrophysiologic phenotype after transient brain ischemia. J Cereb Blood Flow Metab 2005;25:1613–24

59. Lin RC, Matesic DF, Marvin M, et al. Re-expression of the intermediate filament nestin in reactive astrocytes. Neurobiol Dis 1995;2:79–85

60. Eng LF, Ghirnikar RS. GFAP and astrogliosis. Brain Pathol 1994;4: 229–37

61. Norton WT, Aquino DA, Hozumi I, et al. Quantitative aspects of reactive gliosis: A review. Neurochem Res 1992;17:877–85

62. Wilhelmsson U, Li L, Pekna M, et al. Absence of glial fibrillary acidic protein and vimentin prevents hypertrophy of astrocytic processes and improves post-traumatic regeneration. J Neurosci 2004;24:5016–21

63. Zamanian JL, Xu L, Foo LC, et al. Genomic analysis of reactive astrogliosis. J Neurosci 2012;32:6391–410

64. Sabelstrom H, Stenudd M, Reu P, et al. Resident neural stem cells restrict tissue damage and neuronal loss after spinal cord injury in mice. Science 2013;342:637–40

65. Barnabe-Heider F, Goritz C, Sabelstrom H, et al. Origin of new glial cells in intact and injured adult spinal cord. Cell Stem Cell 2010;7: 470–82

66. Magnusson JP, Goritz C, Tatarishvili J, et al. A latent neurogenic program in astrocytes regulated by Notch signaling in the mouse. Science 2014;346:237–41

67. Carlen M, Meletis K, Goritz C, et al. Forebrain ependymal cells are Notch-dependent and generate neuroblasts and astrocytes after stroke. Nat Neurosci 2009;12:259–67

68. Sailer MH, Gerber A, Tostado C, et al. Non-invasive neural stem cells become invasive in vitro by combined FGF2 and BMP4 signaling. J Cell Sci 2013;126:3533–40

69. Rugg-Gunn PJ, Cox BJ, Lanner F, et al. Cell-surface proteomics identifies lineage-specific markers of embryo-derived stem cells. Dev Cell 2012;22:887–901

70. Worsdorfer P, Maxeiner S, Markopoulos C, et al. Connexin expression and functional analysis of gap junctional communication in mouse embryonic stem cells. Stem Cells 2008;26:431–39

71. Lacar B, Young SZ, Platel JC, et al. Gap junction–mediated calcium waves define communication networks among murine postnatal neural progenitor cells. Eur J Neurosci 2011;34:1895–905

72. Roybon L, Lamas NJ, Garcia-Diaz A, et al. Human stem cell–derived spinal cord astrocytes with defined mature or reactive phenotypes. Cell Rep 2013;4:1035–48

73. Sirko S, Behrendt G, Johansson PA, et al. Reactive glia in the injured brain acquire stem cell properties in response to sonic hedgehog. Cell Stem Cell 2013;12:426–39

74. Wanner IB, Anderson MA, Song B, et al. Glial scar borders are formed by newly proliferated, elongated astrocytes that interact to corral inflammatory and fibrotic cells via STAT3-dependent mechanisms after spinal cord injury. J Neurosci 2013;33:12870–86

75. Rivera-Zengotita M, Yachnis AT. Gliosis versus glioma?: Don't grade until you know. Adv Anat Pathol 2012;19:239–49

76. Venere M, Fine HA, Dirks PB, et al. Cancer stem cells in gliomas: Identifying and understanding the apex cell in cancer's hierarchy. Glia 2011;59:1148–54

77. Singh SK, Clarke ID, Hide T, et al. Cancer stem cells in nervous system tumors. Oncogene 2004;23:7267–73

78. Krishnan H, Ochoa-Alvarez JA, Shen Y, et al. Serines in the intracellular tail of podoplanin (PDPN) regulate cell motility. J Biol Chem 2013;288:12215–21

79. Shindo K, Aishima S, Ohuchida K, et al. Podoplanin expression in cancer-associated fibroblasts enhances tumor progression of invasive ductal carcinoma of the pancreas. Mol Cancer 2013;12:168

80. Hoshino A, Ishii G, Ito T, et al. Podoplanin-positive fibroblasts enhance lung adenocarcinoma tumor formation: Podoplanin in fibroblast functions for tumor progression. Cancer Res 2011;71:4769–79

81. Chandramohan V, Bao X, Kato Kaneko M, et al. Recombinant anti-podoplanin (NZ-1) immunotoxin for the treatment of malignant brain tumors. Int J Cancer 2013;132:2339–48

82. Ochoa-Alvarez JA, Krishnan H, Shen Y, et al. Plant lectin can target receptors containing sialic acid, exemplified by podoplanin, to inhibit transformed cell growth and migration. PLoS One 2012;7:e41845

83. Kato Y, Vaidyanathan G, Kaneko MK, et al. Evaluation of anti-podoplanin rat monoclonal antibody NZ-1 for targeting malignant gliomas. Nucl Med Biol 2010;37:785–94

84. Kato Y, Kaneko MK, Kuno A, et al. Inhibition of tumor cell–induced platelet aggregation using a novel anti-podoplanin antibody reacting with its platelet-aggregation–stimulating domain. Biochem Biophys Res Commun 2006;349:1301–7